NiO/nGO photocatalyst for degrading Remazol Golden Yellow (RGY) irradiated by visible and sun lights

Rudy Situmeang [1] and Arya Sanda[1]

[1] Department of Chemistry, University of Lampung, Lampung Province, Indonesia
rudy.tahan@fmipa.unila.ac.id

Abstract. Photocatalysis due to degrading the dyes pollution without give a negative impact on the environment is really interesting. To study the photodegradation, the NiO/nGO catalysts with the ratio of NiO to nGO 0.125/1, 0.250/1 and 0.5/1, were prepared respectively using the gel sol method. Then, the characterization is done such as the X-Ray Diffraction (XRD) method showed that all ratio catalysts had two crystalline phases, n-GO and NiO. The crystalline sizes are 5.45, 8.46, and 17.56 nm, respectively. Infrared spectra of the samples showed the formation of Ni-O and C-OH functional groups. The SE micrograph indicated that the catalysts contained Ni, O, C, and H elements and had agglomeration. The band-gap energy of the catalysts is 1.52, 1.50, and 1.63 eV as a follow as the ratio. The experiment proved that all catalyst was active and successfully reduced the RGY by 90 and 80 % at the exposure time of 120 minutes, using a visible lamp source and that of 41% using sunlight.

Keywords: NiO/nGO, photodegradation, Remazol golden yellow.

1 Introduction

Efforts to deal with water pollution from textile dyes have been carried out in various ways. Starting from conventional methods, for example adsorption using activated carbon [1] and zeolite [2,3] or active sand [4], to advanced methods such as biodegradation [5], ozonolysis [6] and sonolysis [7]. However, both of these methods each have weaknesses and disadvantages. It is hoped that the photocatalytic degradation method using semiconductor materials can be an alternative choice.

Photocatalysis utilizes energy originating from light (sunlight or UV lamp) to activate the catalysis process on the surface of a semiconductor material so that hydroxyl radicals are produced which will degrade organic pollutants and dyes [8]. Some examples of photocatalytic degradation use TiO_2 nanocatalyst which is able to degrade methylene blue by

S. Hadi et al. (eds.), *Proceedings of the 5th International Conference on Applied Sciences, Mathematics, and Informatics (ICASMI 2024)*, Advances in Physics Research 13,
https://doi.org/10.2991/978-94-6463-730-4_16

90.94% with UV light and 94.43% with sunlight for 75 minutes [9]. Furthermore, the $Ni_1V_{1-x}Fe_2O_4$ spinel catalyst was able to degrade RGY by 45% with sunlight in 100 minutes of exposure [10].

Herein, we report the influence of NiO amount in the NiO/nGO on its RGY photodegradation activities using the visible- and sun lights at different times of exposure.

2. Experimental Section

2.1. Materials. The ingredients used are nickel nitrate hexahydrates (Merck, 99%), sodium nitrate, $FeCl_3.6H_2O$ (Merck^{TM}), 1 M and 5% chloride acids, concentrated sulphate acid (Merck^{TM}), potassium permanganates (Merck^{TM}), hydrogen peroxide 30%, aqueous ammonia (pH = 12) (Merck^{TM}), weevil pectin corn, pH indicator, Hydrogen gas (BOC 99.99%), and Remazol Golden Yellow (RGY)

2.2. Instrumentations. X-ray diffractometer (XRD), SE Micrograph and EDX, DR Spectrophotometer, FTIR (Shimadzu IR Prestige 21), Surface Area Analyzer BET (Nova 4200e), ultrasonic apparatus (D68H). UV-Vis Spectrophotometer (Shimadzu Cary- 100).

2.3. Preparation of NiO/nGO. This nanocatalyst was made by adding nickel nitrate solution using an infusion tool into the dissolving pectin solution. The mixture was then stirred using a magnetic stirrer at room temperature until a homogeneous solution was obtained. After adding ammonia and stirring until homogeneous, then the mixture was heated using a hot plate magnetic stirrer at a temperature of 70-80^{o}C until a gel forms. The next step is freeze drying process and calcination [11]. The catalyst powder obtained was crushed until smooth using agate mortar and continued for characterization. The catalyst powder obtained was then impregnated with nGO. The impregnation was carried out in a ratio of (1/0.125), (1/0.25) and (1/0.5), respectively. Finally, the catalyst characterization is carried out.

3. Characterization of NiO/nGO

3.1. X-ray diffraction analysis. The diffractograms of the sample were measured from $2\theta = 10°$ to 80° on a Philips diffractometer Model PW 1710 using Cu Kα radiation at step 0.02° per second. The phase identification was performed using the search and match method. The sample pattern is compared to those of the standards in the JCPDF. Then, the crystalline size was also determined using the Scherrer method [12].

3.2. FTIR spectra analysis. The procedure to analyse the sample which is treated firstly by heating at 80°C and vacuumed in a desiccator as mentioned on Situmeang et al., 2022 [13] using IR Prestige-21 Shimadzu instrument.

3.3. SEM-EDX analysis. The 0.1 g sample is placed in a sample container containing copper sticking tape, then the sample is coated with a thin layer of gold or a conductive material other. Then the sample is given an electron beam. Electron beam will be reflected by the sample and then captured by the detector to form a photo [14].

3.4. Band gap energy analysis. To measure the band-gap energy of the NiO/nGO samples, a certain quantity of the sample was analyzed using UV-Vis Diffuse Reflectance Spectroscopy and scanned over the wavelength in the range of 200-800 nm [15].

3.5. Activity tests. In this research, 0.1 g of NiO/nGO nanocomposite and 15 ppm of RGY were used. The photocatalytic activity test on the NiO/nGO nanocomposite was carried out on the RGY compound by mixing 0.1 gr of NiO/nGO nanocomposite into 150 mL of RGY with a concentration of 15 ppm into a beaker, then homogenized. Then, the experimental steps follow the previous procedures [13], . The same thing was done with various time variations, namely 60;80; 100 and 120 minutes.

4. Result and Discussion

4.1. X-ray diffractogram analysis. As shown in Figure 1 below, the crystalline phase of NiO formed with the presence of four typical diffraction peaks at the angles of 2θ = 43.24; 37.21; 62.80 ; and 44.4. Those peaks are in accordance with the data of COD 01-073-1523. Further analysis using Debye Scherrer calculation, it is proved that the NiO catalyst has a crystalline size of 6.03 nm.

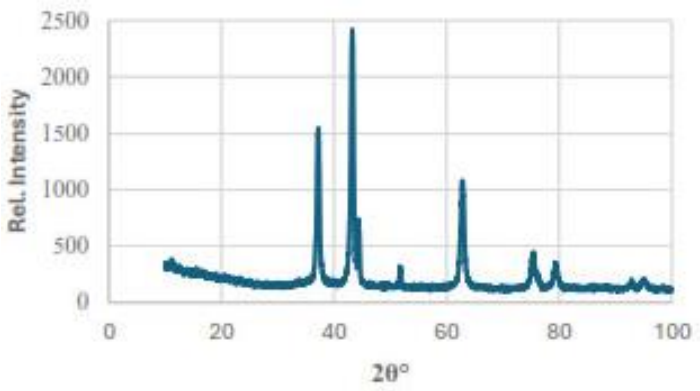

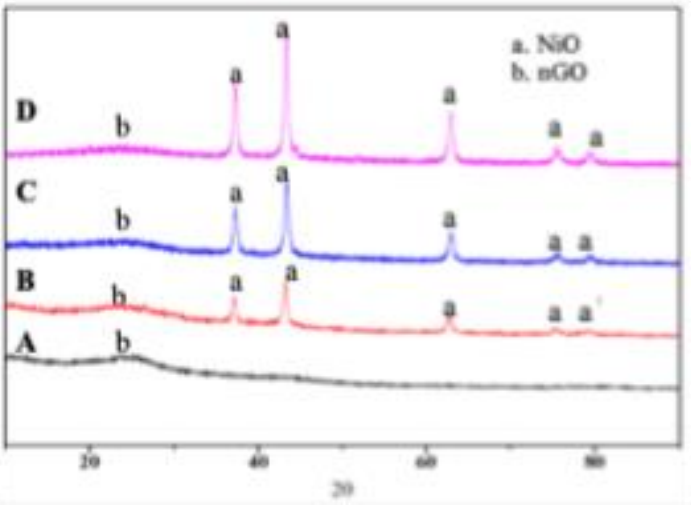

Figure 1. Diffractogram of NiO prepared (above) and NiO/nGO (below) with the ratio of 0.125/1(B), 0.25/1(C), 0.5/1(D), and nGO (A), respectively.

In the diffractogram of NiO/nGO (Figure 1), NiO phase is observed as the sharp peaks and well distributed on nGO while the ratio of NiO to nGO increased. It is proved that the peak of nGO at 23.52° becomes flatter as the amount of NiO on nGO increased. Furthermore, the crystalline sizes of NiO impregnated into nGO with ratios of 0.125, 0.25, and 0.5 and calculated using the Debye-Scherrer method were obtained respectively of 5.46, 8.12, and 17.56 nm.

4.2. FTIR spectra analysis

Analysis of the functional groups of the NiO/nGO catalysts using FTIR to find out the interaction that occur between the bonds of NiO and nGO molecules. Determination of bond type is observed by looking at the maximum absorption in the infrared spectrum generated. The FTIR spectra of the catalysts are shown in Figure 2.

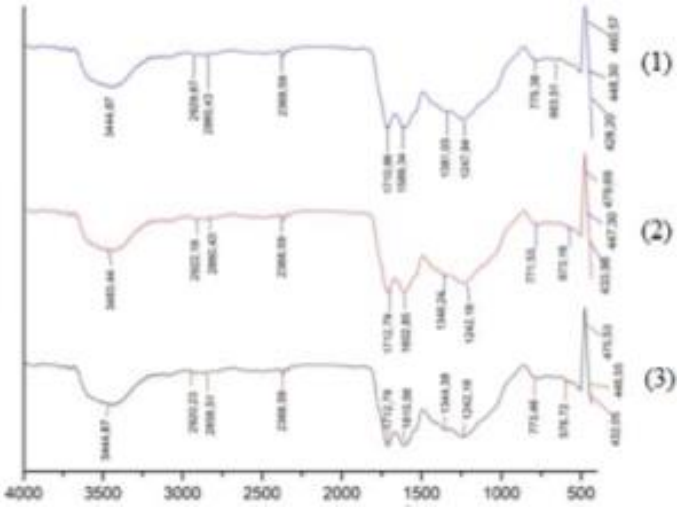

Figure 2. Spectra of NiO/nGO with ratio of 0.125 (1), 0.25 (2), and 0.5 (3)

Based on Figure 2, the results of the infrared spectrum of the NiO/nGO catalyst were observed at wavelengths of 4000-400 cm^{-1}. Then, it was found that the wavenumber of 3444.87 and 3483.44 cm^{-1} indicates the presence of O-H stretching vibrations of water molecules adsorbed by catalysts from the environment due to the very nature of the catalyst porous [16]. At the wavenumber of 2929.87 – 2368.59 cm^{-1}, it shows C-C stretching vibrations which are thought to originate from the natural surface of graphite that was not successfully oxidized on graphene oxide. The wavenumber of 1712.79 and 1710.86 cm^{-1} represented the weak absorption C=O stretching vibration of –COOH in graphene oxide, respectively. The wavenumber of 1589.34 –1610.56 cm^{-1} is the peak of the C=C bending vibration that shows the presence of aromatic compounds and wave numbers of 1348.24-1242.16 cm^{-1} shows the C-OH stretching vibration which overlaps with that of the C-O group [17]. The wave number region of 775.38–576.72 cm^{-1} exists C-C stretching vibrations from the natural surface of graphite. In the wave number region of 428.20–479.69 cm^{-1}, it is suspected the bending vibrations of the Ni-O occurred. This is in accordance with the reference which states that the bending vibration of the Ni-O bond in the absorption band 480-200 cm^{-1} [18].

4.3. SEM-EDS analysis. Micrographs and elemental analysis were carried out on NiO/nGO with a ratio of 0.125. The analysis results in Figure 3 state that NiO is distributed unevenly on the nGO surface and agglomeration is visible.

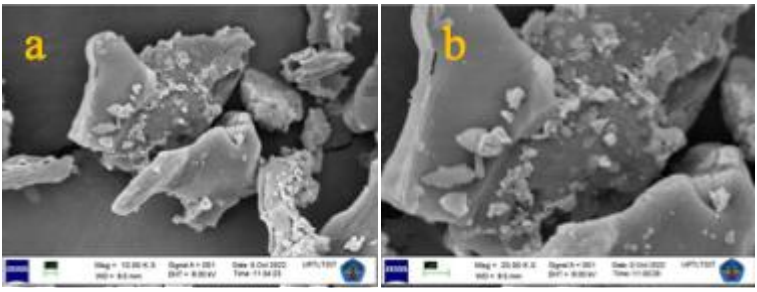

Figure 3. SE Micrograph of NiO/nGO at the ratio of 0.125 with the magnification of 1500x (a) and 2000x (b)

Next, EDX data is shown in Figure 4 below,

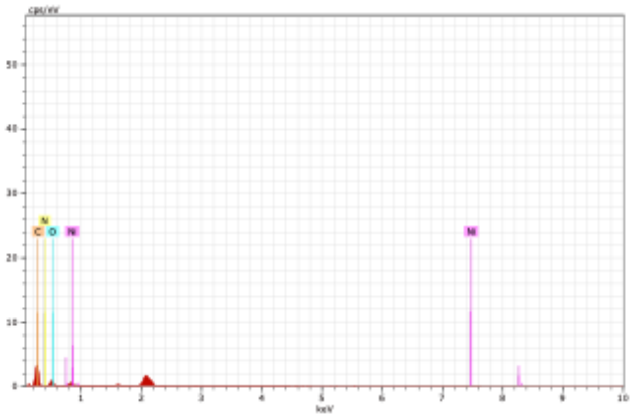

Figure 4. Spectra EDX of NiO/nGO with the ratio of 0.125

Furthermore, by using the element percentage data in the EDX data with the percentage ratio of 10.49:22.98:63.66, we obtained a Ni:O:C ratio (in mole) of 2.27:4.35:9.18 so that if a comparison between nickel and oxygen is made, it appears that oxygen is greater. This is because oxygen not only bonds with nickel atoms but also with graphene oxides. In addition, nitrogen was also found.

4.4. Band gap energy analysis. Band-gap energy analysis (Eg) of the NiO catalyst was carried out using DRS (Diffuse Reflectance UV-VIS Spectroscopy) instrumentation. Basic principles this method is quite simple, namely if the material is illuminated with waves electromagnetic then photons will be absorbed by electrons in the material. Generally, the use this tool to determine the band gap energy of photocatalysts or semiconductors is apparently a simple way[19].

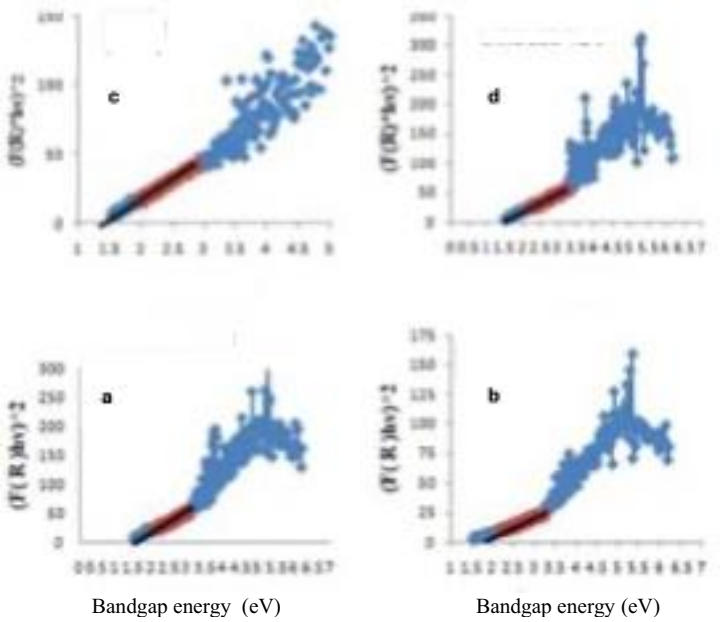

Figure 5. Band gap energy of NiO/nGO determined graphically.

Based on Figure 5, the band-gap energy for the prepared catalyst namely nGO (c); 0.125 NiO/nGO (d); 0.25 NiO/nGO (a); 0.5 NiO/nGO (b) ; and NiO, is 1.42, 1.52, 1.50, 1.63, and 3.11 eV, respectively. The band-gap energy clearly tends to increase while the amount of NiO dopant increases, but this value is still below 2.0 eV so that it can be active as a photocatalyst in the visible region [20].

4.6. UV-Vis Spectra analysis

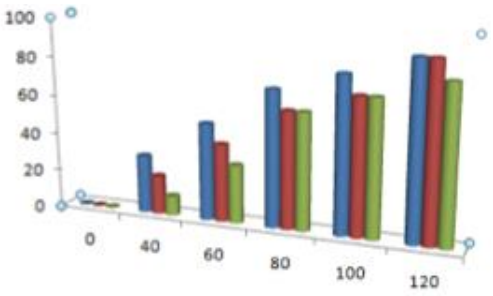

Figure 6. Remazol Golden Yellow (RGY) Degradation Percentage with Catalyst NiO/n-GO of 0.125/1(blue), 0.25/1 (red) and 0.5/1 (green) irradiated by visible light.

In Figure 6, it shows the relationship between exposure time and percent degradation of RGY by the NiO/nGO catalysts with the mark of blue, red and green, respectively.

Degradation percentage of the RGY in the ratio of 0.125 (blue) increased linearly at the concentrations of 80% and 90% depending on the exposure time applied. The degradation percentage of the RGY in the ratio of 0.25 (red) experienced a linear increase of 70% and 90% on the exposure time of 100 and 120 minutes respectively. while the degradation percentage of the RGY sample in the ratio of 0.5 (green) experienced an increase in linear speed of 70% and 80% using visible light irradiation.

Results of percentage comparison of RGY Degradation using the NiO/nGO (0.125/1) Catalyst Irradiated by UV and sun lights is shown in Figure 7 below. The percentage comparison of the RGY degradation using UV and Sun lights is shown that the percentage result of RGY degradation is lower using sun light than that of using UV light. In addition, the percentage of RGY degradation using sun light increased exponentially with the augmented exposure time. It is 41% RGY degradation at 120 minutes exposure time.

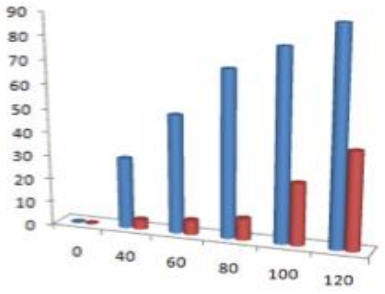

Figure 7. Percentage comparison of RGY Degradation using the NiO/nGO (0.125/1) Catalyst Irradiated by UV and sun lights. (Notes : blue = irradiated by UV light, red= irradiated by sunlight)

5. Conclusion

Based on the research that has been carried out, conclusions can be drawn that: (1). The crystalline phase formed in each ratio of NiO/nGO with an average catalyst crystalline size of 5.46; 8.46 and 17.56 nm, respectively, (2). The results of DRS analysis showed that the band-gap energy of NiO was (3.11 eV); nGO (1.42 eV) and NiO/nGO 1st variation (1.52 eV); 2nd variation (1.50 eV); and 3rd variation (1.63 eV), (3). The analysis of FTIR spectra showed the formation of Ni-O and C- OH functional groups at wave numbers 428.20 and 1348.24 cm^{-1}. (4). All catalysts prepared is active to degrade RGY with the maximum result

of 90% using UV light irradiation, and 41% using sun light with the exposure time of 120 minutes.

References

1. Shen, Zhemin., Wang, Wenhua., Jia, Jinping., Ye, Jianchang., Feng, Xue., and Peng, An. : Degradation of dye solution by an activated carbon fiber electrode electrolysis system. J. Hazard. Mat., **84**(1), 107 – 116 (2001).

2. Aleksic, M., Koprivanac, N., Lonèaric Bozic, A., and Kušic, H.: The Potential of Fe-exchanged Y Zeolite as a Heterogeneous Fenton-type Catalyst For Oxidative Degradation of Reactive Dye in Water. Chem. Biochem. Eng. Q., **24**(3), 309 –319 (2010).

3. Franciscon, E., Grossman, M. J., Paschoal, J. A. R., Reyes, F. G. R., and Durrant, L. R.: Decolorization and biodegradation of reactive sulfonated azo dyes by a newly isolated Brevibacterium sp. strain VN-15. SpringerPlus, **1**(37), 1 -10 (2012).

4. Šíma, Jan., and Hasal, Pavel.: Photocatalytic Degradation of Textile Dyes in a TiO_2/UV System. Che. Eng. Trans., **32**, 79 – 84 (2013).

5. Isha., Verma, Anoop., and Kumari, Shilpi.: Synergistic effects of sonolysis combined with photocatalysis in degradation of industrial waste water. Int. J. Env. Scie. : Development and Monitoring, **4**(2), 10 – 12 (2013).

6. Manurung, P., Situmeang, R., Ginting, E., and Pardede, I.: Synthesis and Characterization of titania-rice husk silica composites as photocatalyst, Indones. J. Chem., **15**(1), 36 – 42 (2015).

7. Glienke, J., Schillberg, W., Stelter, M., Braeutigam, P.: Prediction of degradability of micropollutants by sonolysis in water with QSPR - a case study on phenol derivates. Ultrasonics Sonochemistry. **82**, 105867 (2022).

8. Khan, S., Noor, T., Iqbal, N., and Yaqoob, L.: Photocatalytic Dye Degradation from Textile waste water: A Review. ACS Omega 9, 21751 – 21767 (2024).

9. Ajmal, A., Majeed, I., Malik, R. N., Idriss, H., and Nadeem, M. A.**:** Principles and mechanisms of photocatalytic dye degradation on TiO_2 based photocatalysts: a comparative overview. RSC Advances **4**, 37003-37026 (2014).

10. Situmeang, R., Romiyati, R., Saputra, A.A., and Sembiring, S.: $Ni_{0.5}V_{0.5}Fe_2O_4$ Nanophotocatalyst: Preparation, Characterization, and its activity on Remazol Golden Yellow Degradation under sunlight irradiation, Key Engineering Materials, **840**, 71 – 78 (2020).

11. Beckham, G.T., Matthews, J.F., Peters, B., Bomble, Y.J. Himmel, M.E., and Crowley M.F.: Molecular-Level Origins of Biomass Recalcitrance: Decrystallization Free Energies for Four Common Cellulose Polymorphs, J. Phys. Chem. B, **115**(41), 4118 – 4127 (2001).

12. Situmeang, R., Supryanto, R., Kahar, Lolita N.A., Sukartiningsih, L. A., Simanjuntak, W., and Sembiring, S.: Characteristics of Nano-Size $LaCrO_3$ Prepared Through Sol-Gel Route Using Pectin as Emulsifying Agent, Oriental Journal of Chemistry **33**(4), 1705-1713 (2017).

13. Situmeang, R., Romiyati, R., R., and Yuwono, S. D., Manurung, P., Firdaus, I., and Sembiring, S.: The effect of vanadium addition in Ni $_{1-x}$ V$_x$ Fe$_2$O$_4$ nano photocatysts on remazol golden yellow degradation under visible light irradiation. *Advances in Natural Sciences:Nanoscience and nanotechnology*, **13**(3), 35024 (2022).

14. Hartanto, and Ratnawati, R.: Pembuatan Karbon Aktif Dari Tempurung Kelapa Sawit Dengan Metode Aktifitas Kimia. Jurnal Sains Materi Indonesia **12**(1), 12-16 (2018).

15. Hussain, M. M., Rahman, M. M., Asiri, A. M.: Ultrasensitive and selective 4-aminophenol chemical sensor development based on nickel oxide nanoparticles decorated carbon nanotube nanocomposites for green environment. Journal of Environmental Sciences **53,** 27–38 (2017).

16. Oya, A. dan Marsh, H.: Review Phenomena Of Catalytic Graphitization, Journal Of Materials Science, **17**(2), 39-45 (1982).

17. Choucair, P. Thordarson, J. A. Stride. Gram-Scale Production of Graphene Based on Solvothermal Synthesis and Sonication. Natural Nanotechnol. **4**, 30–33(2009).

18. Azharudeen, A. M., Karthigaa, R., Rajarajan, M., Suganthi A.: Fabrication, characterization of polyaniline intercalated NiO nanocomposites and application inthe development of non-enzymatic glucose biosensor, Arabian Journal of Chemistry **13**, 4053–4064 (2020)

19. Hsiao, C., Liao, S., Yen, M., Liu, P., Pu, N., Wang, C., Ma. C.: Preparation of Covalently Functionalized Graphene Using Residual Oxygen-Containing Functional Groups. American Chemical Society. **2**(11), 3092– 3099 (2010).

20. Casbeer, E., Sharma, V. K., and Li, X.-Z.: Synthesis and photocatalytic activity of ferrites under visible light: a review. Separation and Purification Technology 87, 1–14 (2012).